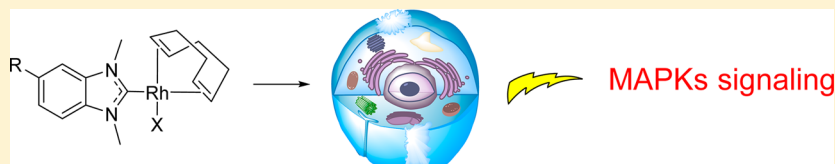


Rhodium(I) N-Heterocyclic Carbene Bioorganometallics as in Vitro Antiproliferative Agents with Distinct Effects on Cellular Signaling

Luciano Oehninger,[†] Sarah Spreckelmeyer,[†] Pavlo Holenya,[‡] Samuel M. Meier,[§] Suzan Can,[‡] Hamed Alborzina,[‡] Julia Schur,[†] Bernhard K. Keppler,^{||} Stefan Wölfl,[‡] and Ingo Ott^{*,†}[†]Institute of Medicinal and Pharmaceutical Chemistry, Technische Universität Braunschweig, Beethovenstraße 55, D-38106 Braunschweig, Germany[‡]Institute of Pharmacy and Molecular Biotechnology, Ruprecht-Karls-Universität Heidelberg, Im Neuenheimer Feld 364, D-69120 Heidelberg, Germany[§]Department of Analytical Chemistry, University of Vienna, Waehringer Straße 38, 1090 Vienna, Austria^{||}Institute of Inorganic Chemistry, University of Vienna, Waehringer Straße 42, 1090 Vienna, Austria

Supporting Information



ABSTRACT: Organometallics with N-heterocyclic carbene (NHC) ligands have triggered major interest in inorganic medicinal chemistry. Complexes of the type Rh(I)(NHC)(COD)X (where X is Cl or I, COD is cyclooctadiene, and NHC is a dimethylbenzimidazolylidene) represent a promising type of new metallodrugs that have been explored by advanced biomedical methods only recently. In this work, we have synthesized and characterized several complexes of this type. As observed by mass spectrometry, these complexes remained stable over at least 3 h in aqueous solution, after which hydrolysis of the halido ligands occurred and release of the NHC ligand was evident. Effects against mitochondria and general cell tumor metabolism were noted at higher concentrations, whereas phosphorylation of HSP27, p38, ERK1/2, FAK, and p70S6K was induced substantially already at lower exposure levels. Regarding the antiproliferative activity in tumor cells, a clear preference for iodido over chlorido secondary ligands was noted, as well as effects of the substituents of the NHC ligand.

INTRODUCTION

Organometallic complexes have been emerging as promising new metallodrug candidates and hold great promise in particular for cancer chemotherapy.^{1–3} Among the most frequently studied types, N-heterocyclic carbene (NHC) complexes with gold and silver as central atoms have demonstrated fascinating biochemical properties as enzyme inhibitors and antimetabolic agents, suggesting possible applications in the therapy of tumors or infectious diseases.^{4–6} Early reports^{7–9} demonstrate that various metals other than silver or gold can be successfully used to generate biologically active metal NHC complexes; however, only during the past few years has this particular field of bioorganometallic chemistry been gradually extended to different metals including platinum,^{10–12} ruthenium,¹³ iridium,^{14,15} and rhodium.^{15–17}

Although Rh(I) NHC complexes were among the first metal NHC complexes to be synthesized, with biological (antibacterial) activity reported in 1996,⁸ it was not until 2013 that their promising potential as anticancer metallodrugs was described in more detail in three further reports by Simpson et al.,¹⁵ McAlpine and co-workers,¹⁶ and us¹⁷ (see Figure 1 for examples). The use of the Rh(I) center is of special interest because Rh(I) is isoelectronic with Pt(II), and both ions form

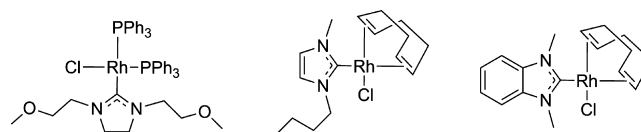


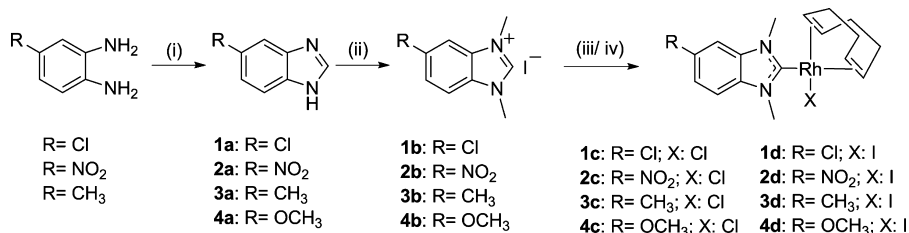
Figure 1. Examples of previously biologically studied rhodium(I) NHC complexes.^{8,9,16,17}

complexes with square-planar geometries. Accordingly, some analogies with the clinically used platinum drugs are evident, and in fact, interaction with DNA was found to be a likely mode of drug action also for Rh(I) NHC complexes.¹⁶

Rhodium(III) complexes with ligands other than NHCs (e.g., polypyridyls, staurosporine) have been studied by Sheldrick and co-workers,^{18,19} Meggers and co-workers,²⁰ Leung and Ma and co-workers,^{21,22} Che and co-workers,²³ and others.^{24,25} Depending on the coordinated ligands for these complexes, several targets were confirmed, including protein kinases, other enzymes (e.g., the ubiquitin–proteasome system), and DNA.

Received: July 23, 2015

Published: November 23, 2015

Scheme 1. Synthesis Procedure for the (COD)Rhodium(I) Derivatives^a

^a(i) Formic acid, reflux, 12 h; (ii) alkylhalide, K₂CO₃, CH₃CN, reflux, 6 h; (iii) Ag₂O in CH₂Cl₂, 4 h; (iv) bis[halido(η^2,η^2 -cycloocta-1,5-diene)rhodium(I)], 2 h.

In this article, we report on interesting chemical-biological properties that we have observed using Rh(I) complexes **1c/d**–**4c/d** of the type Rh(I)(NHC)(COD)X (where X is Cl or I, COD is cyclooctadiene, and NHC is a dimethylbenzimidazolylidene; see Scheme 1). The dimethylimidazolylidene NHC fragment was identified as a useful organometallic ligand for obtaining cytotoxic complexes of this general type in our recent report.¹⁷ Initially, the effects of model complexes containing a 5-nitrobenzimidazole-based NHC ligand and chlorido or iodido secondary ligands (complexes **2c** and **2d**) were evaluated. In these compounds, the electron-withdrawing nitro group reduces the donor capacity of the NHC ligand, and this should, in turn, facilitate ligand-exchange interactions with biomolecular targets. Compounds **2c** and **2d** can thus be regarded as model compounds with higher chemical reactivities and were therefore used to investigate important effects of the compound type. In a further step, the effects of different substituents on the 5-position of the NHC ligand on tumor cell proliferation inhibition were evaluated (**1c/d**, **3c/d**, and **4c/d**).

CHEMISTRY

Complexes **1c/d**–**4c/d** were obtained starting from the respective substituted 1,2-diaminobenzenes or benzimidazoles (Scheme 1). Ring closure of the diaminobenzenes with formic acid afforded the benzimidazoles **1a**–**3a**. Benzimidazole **4a** was commercially available. Next, benzimidazolium cations **1b**–**4b** were formed by alkylation using methyl iodide in the presence of K₂CO₃. Finally, complexes **1c/d**–**4c/d** were conveniently obtained by activation of the respective benzimidazolium cations with Ag₂O and subsequent transmetalation using bis[halido(η^2,η^2 -cycloocta-1,5-diene)rhodium(I)]. The target compounds were purified by filtration over Celite and recrystallized from a mixture of CH₂Cl₂ and *n*-hexane. Nuclear magnetic resonance (NMR) and mass spectrometry (MS) spectra confirmed the suggested structures, and elemental analyses indicated their high purities.

The target complexes give well-resolved NMR spectra, as discussed here for **4c** and **4d** as examples (see Figure 2). In the ¹H NMR spectra of **4c** and **4d**, the shifts of the signals of the respective methoxy groups (b in Figure 2) show no difference, whereas the N–CH₃ protons (a in Figure 2) of the iodido derivative **4d** are shifted slightly upfield compared to **4c**. This phenomenon can be explained by the difference in the electronic densities of the halido ligands. The cis- (c in Figure 2) and trans- (d in Figure 2) positioned olefinic signals (cis/trans relative to X) of the COD moiety are shifted slightly downfield in the iodido derivative **4d**. However, the most obvious effect observed in the spectra of these derivatives is the splitting of some of the CH₂ signals (e in Figure 2) in complex **4d**. The iodido ligand has a larger volume than the chlorido

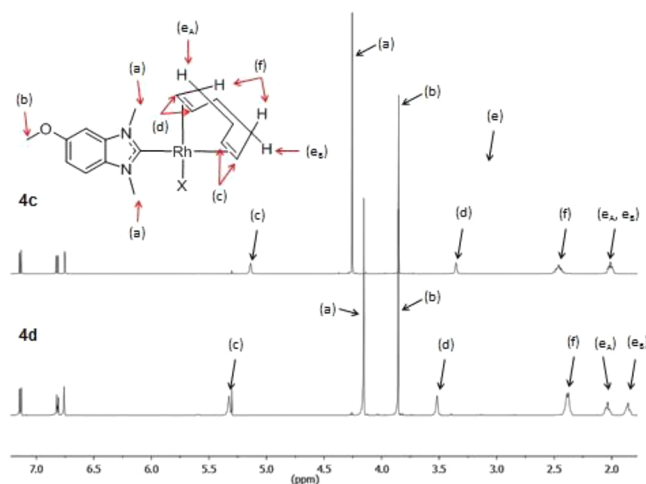


Figure 2. ¹H NMR spectra of (top) **4c** (X = Cl) and (bottom) **4d** (X = I) in CDCl₃. (a) N–CH₃, (b) O–CH₃, (c) trans CH of COD, (d) cis CH of COD, (e_A) pseudoequatorial CH₂ of COD in cis position, (e_B) pseudoequatorial CH₂ of COD in trans position, (f) pseudoaxial CH₂ of COD.

ligand, resulting in a greater steric hindrance toward the CH₂ protons in proximity, and this difference in the electronic surroundings of the protons presumably led to the splitting of the pseudoequatorial (e_A and e_B) signals. The same effect was observed with the couples **1c/d**–**3c/d**.

MASS SPECTROMETRY: HYDROLYTIC STABILITY

Electrospray ionization ion-trap mass spectrometry (ESI-IT MS) was used to study the stability and reactivity of **2c** and **2d**. For this purpose, the compounds were dissolved in dimethyl sulfoxide (DMSO) or dimethylformamide (DMF) (10 mM concentration), diluted to 100 μ M with water, and incubated at 37 °C in the dark, and aliquots withdrawn after different incubation periods were investigated.

Compound **2c** is stable for 3 h, irrespective of whether the solvent is DMSO and DMF, which suggests that these solvents do not influence the stability of **2c**. After 6 and 24 h, the mass spectra in positive-ion mode of **2c** dissolved in DMSO and DMF were very similar. As evidenced by the mass signal corresponding to [LRh(COD)(OH) – H]⁺, where L is the nitro-NHC ligand and COD is cyclooctadiene, the compound hydrolyzes the Rh–Cl bond and forms either aqua or hydroxido complexes. Loss of the NHC ligand was observed and seemed to become more pronounced at longer incubation times, whereas the COD ligand remained coordinated. The protonated NHC ligand was detected at *m/z* 192.05 (*m*_{theor} = 192.08). Moreover, nonselective solvent adducts with the

organometallic compound were observed for both DMF and DMSO. Increasing the dry temperature in the ESI source from 180 to 300 °C did not reduce either the DMSO or DMF adducts, but led to enhanced loss of the NHC ligand. Nonselective solvent adducts are indicated by broad signals in the mass spectrum compared to the sharp coordinated adducts; for example, Figure 3 shows the broad nonselective solvent

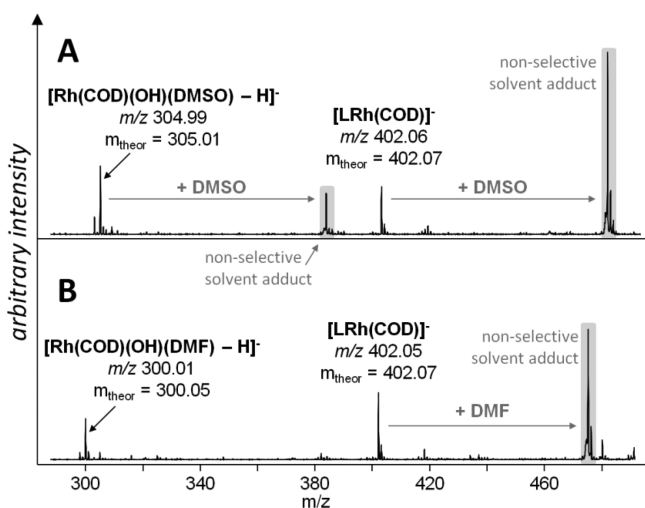


Figure 3. Sections of the ESI-IT mass spectra in positive-ion mode of **2c** showing the different types of solvent adducts with (A) DMSO and (B) DMF. Broad mass signals indicate nonselective adducts between the solvent and metal, and sharp peaks indicate solvent coordination to the metal.

adduct of hydrolyzed **2c** at m/z 480.06 and the respective complex giving a sharp mass signal at m/z 402.06. The negative-ion mode spectra of **2c** dissolved in DMSO and DMF feature a single mass signal that increases over time and corresponds to a dimeric Rh complex that has undergone carbene release, namely, $[\text{Rh}_2(\text{COD})_2(\mu\text{-Cl})_3(\text{OH})_2 - 2\text{H}]^-$ (Figure S1B, Supporting Information). Rhodium has a strong affinity for chloride, and a similar type of Rh-chlorido dimer was reported that was also accompanied by ligand release.²⁶

Compound **2d** is also stable for 3 h in DMF and DMSO, after which increases in free carbene and $[\text{Rh}(\text{COD})(\text{OH})-$

$(\text{DMSO}) - \text{H}]^+$ were observed in positive-ion mode. Generally, the iodido analogue **2d** undergoes very similar hydrolysis processes, giving mass signals virtually identical to those of **2c** (Scheme 2). The compound hydrolyzes slightly faster and forms aqua or hydroxido complexes again corresponding to $[\text{LRh}(\text{COD})(\text{OH}) - \text{H}]^+$. However, release of the NHC ligands seems slightly more pronounced for **2d**. The mass spectra of both the DMSO and DMF solutions in negative-ion mode revealed two major signals at m/z 480.82 and 605.05. MS/MS experiments of these mass signals did not reveal any additional information on their identity. Furthermore, mass signals corresponding to I^- and I_3^- were detected, supporting the hypothesis of the hydrolysis pathways.

Of note is the mass signal at m/z 509.96, which was found in the positive-ion mass spectra of **2c** and **2d** with DMSO after >6 h of incubation. The identity of the parent mass signal is unclear, but MS/MS experiments revealed a fragment corresponding to $[\text{LRh}(\text{OH})(\text{DMSO})_2 - \text{H} + \text{Fu}]^+$, where Fu is an unknown neutral fragment with m/z 44. This mass signal increased over time for both compounds, suggesting that COD release might also represent a possible reaction pathway.

Further details on MS measurements are provided in the Supporting Information.

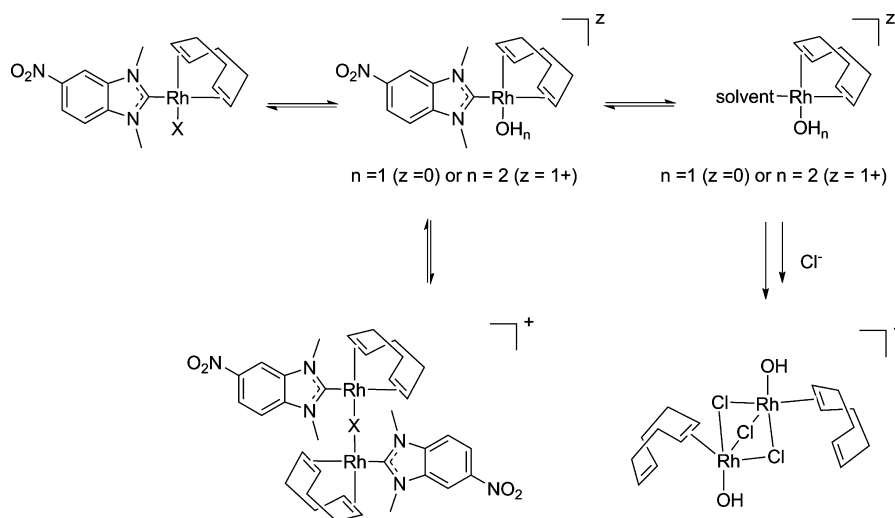
■ EFFECTS ON MITOCHONDRIAL AND CELL METABOLISM

In previous studies on metal NHC complexes, we observed strong effects against mitochondria as well as tumor cell metabolism.^{13,27,28} Analogous experiments with **2c** and **2d** showed some comparable trends (e.g., a decrease of the mitochondrial membrane potential with both compounds, inhibition of cell respiration with **2d**); however, the effects were less evident and appeared significant only at much higher dosages (e.g., 50 μM). A more detailed discussion of these results is presented in the Supporting Information.

■ ELISA MICROARRAYS

To analyze the effects of complexes **2c** and **2d** on cell signaling, enzyme-linked immunosorbant assay (ELISA) microarrays were applied to detect the absolute levels of a selection of key signaling proteins in their phosphorylated states. To obtain time-resolved images of signaling modulation, HT-29 cells were

Scheme 2. Proposed Hydrolysis Pathway of **2c** ($\text{X} = \text{Cl}^-$) and **2d** ($\text{X} = \text{I}^-$) in Aqueous Solution



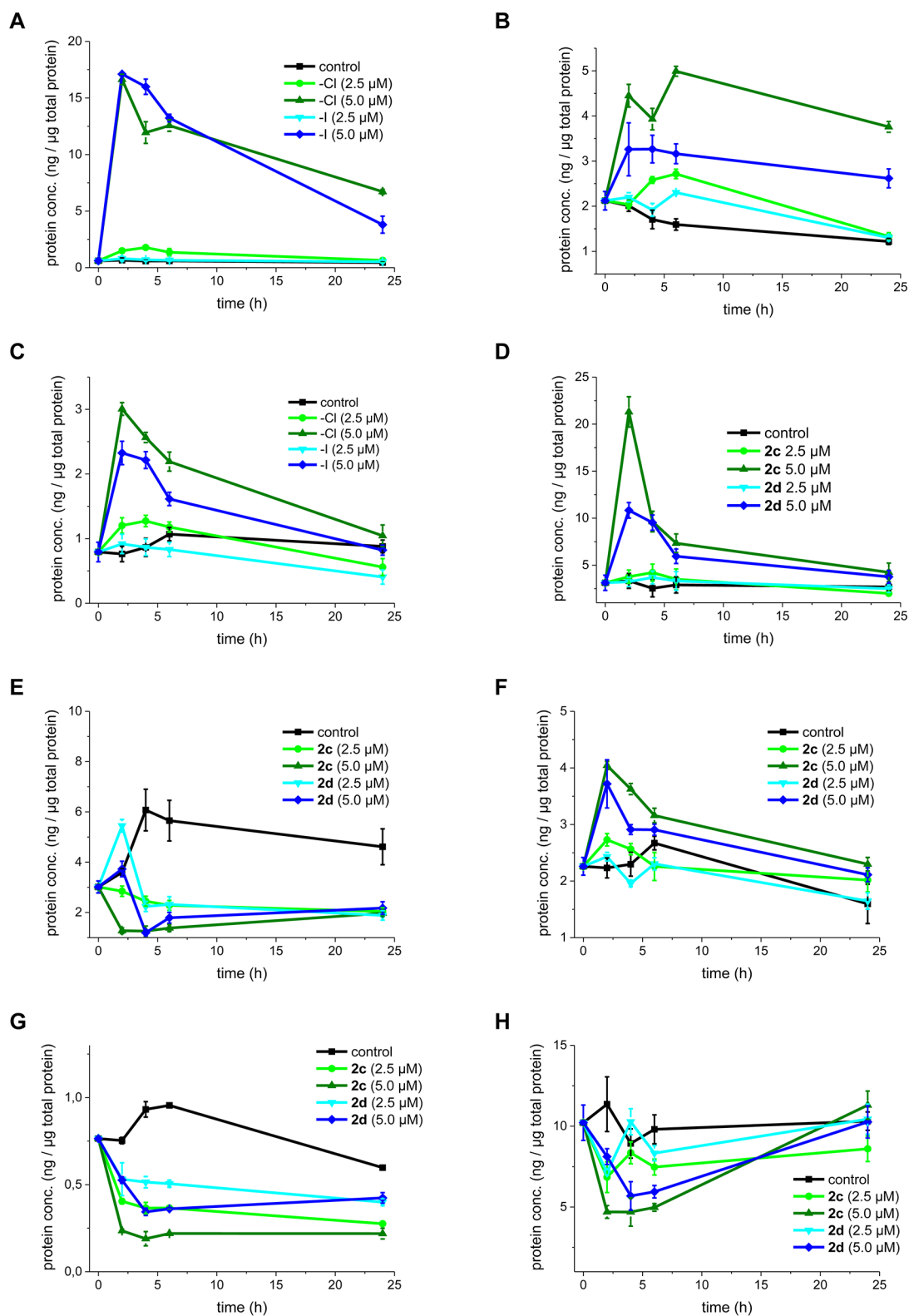


Figure 4. ELISA microarrays with **2c** and **2d**: (A) phospho-HSP27^{S78/S82}, (B) phospho-p38^{T180/Y182} (no legend), (C) phospho-ERK1^{T202/Y204}, (D) phospho-ERK2^{T185/Y187}, (E) phospho-FAK^{Y397}, (F) phospho-p70S6^{T421/S424}, (G) phospho-WNK1^{T60}, (H) phospho-GSK-3β^{S9}.

incubated in time-course experiments (0–24 h) with two concentrations of each compound, namely, 2.5 and 5.0 μM (Figure 4), and cell lysates collected at indicated time points were incubated with the microarrays.

We observed a significant time-dependent activation of mitogen-activated protein kinases (MAPKs). The levels of

phospho-ERK1 (T202/Y204), phospho-ERK2 (T185/Y187), and phospho-p38α (T180/Y182) increased 2–10-fold upon treatment with 5.0 μM **2c** compared to mock-treated (0.1% v/v DMF) samples. The same concentration of **2d** showed slightly weaker effects on MAPK activation. ERK1/2 and p38 are generally known to be activated in response to the intracellular

redox state and oxidative stress and potentially contribute to influencing cell survival or cell death.²⁹

Our analysis also revealed a strong increase of chaperone HSP27 phosphorylation. This protein mediates the protection properties of cells in response to cytotoxic stress (e.g., loss of protein functionality upon binding of organometallic fragments), growth arrest, or receptor-mediated apoptosis.³⁰

Interestingly, phospho-FAK (Y397), known to regulate focal contacts and cell detachment,³¹ exhibited a transient activation profile with both compounds: 5 μ M **2c** and **2d** induced a slight increase in its phosphorylation during 2 h of treatment followed by a sustained decrease. The levels of phospho-p70S6 kinase, a key downstream effector of mTORC1, were also increased upon treatment, indicating changes in cellular protein synthesis.³² Several signaling proteins, among them the key protein of PI3 kinase signaling, Akt1; the important transcription factor CREB; and the DNA damage checkpoint Chk2 showed only minor or insignificant changes in phosphorylation (see [Supporting Information](#)). Finally, we observed a decrease in phosphorylated ERKs signaling upstream modulator WNK1, implicated in antiapoptotic signaling.³³ GSK-3 β was also dephosphorylated (activated) upon treatment. This enzyme is a key regulator of numerous signaling pathways, including cellular responses to Wnt, receptor tyrosine kinases, and G protein-coupled receptors and is involved in glycogen metabolism and cell cycle regulation and proliferation.³⁴

Table 1. Antiproliferative Effects against HT-29 and MDA-MB-231 Cells

	IC ₅₀ HT-29 (μ M)	IC ₅₀ MDA-MB-231 (μ M)
1a	>100	>100
2a	>100	>100
3a	>100	>100
4a	>100	>100
1b	>100	>100
2b	>100	>100
3b	>100	>100
4b	>100	>100
1c	12.1 \pm 1.5	9.0 \pm 0.9
1d	5.1 \pm 0.2	2.7 \pm 1.2
2c	10.2 \pm 2.2	5.2 \pm 0.1
2d	8.6 \pm 0.6	6.4 \pm 1.2
3c	5.2 \pm 1.6	2.4 \pm 0.6
3d	1.5 \pm 0.3	1.5 \pm 0.1
4c	9.5 \pm 0.4	4.1 \pm 0.6
4d	6.6 \pm 0.6	3.5 \pm 0.3

■ ANTIPROLIFERATIVE EFFECTS IN TUMOR CELLS

To evaluate the effects on proliferation inhibition of different substituents on the NHC ligand, we screened complexes containing different donor/acceptor groups against tumor cell lines. Complexes **1c/d–4c/d** along with their respective benzimidazole and benzimidazolium iodide precursors were investigated on two tumor cell lines (namely, HT-29 colon carcinoma and MDA-MB-231 human breast adenocarcinoma). The precursor [Rh(I)Cl(COD)]₂ without NHC ligand is inactive in terms of cytotoxicity, as reported earlier.¹⁷ Whereas the metal free benzimidazoles and benzimidazolium cations **1a/b–4a/b** were not active, the rhodium complexes **1c/d–4c/d** exhibited half-maximal inhibitory concentration (IC₅₀) values in the low micromolar range (1.5–12.1 μ M) with preference for

MDA-MB-231 cells over HT-29 cells. Established anticancer drugs such as cisplatin and 5-fluorouracil trigger comparable cytotoxic effects in the range of approximately 1–10 μ M in this assay.^{35,36} Regarding the substituents on the NHC ligand, the methyl group of **3c/d** triggered the lowest IC₅₀ values in both cell lines, and regarding the secondary halido ligands, the iodido derivatives **1d–4d** were in most cases more active than the respective chlorido complexes **1c–4c**.

■ CONCLUSIONS

Complexes of the type Rh(I)(NHC)(COD)X (where X = Cl or I) can be conveniently prepared following an established method that is based on the reaction of the precursor benzimidazolium cations with Ag₂O and a subsequent transmetalation reaction using bis[halido(η^2, η^2 -cycloocta-1,5-diene)-rhodium(I)]. ¹H NMR spectra confirmed differing electronic effects of the chlorido and iodido ligands, which might indicate different kinetic reactivities. The two organometallic Rh compounds **2c** and **2d** were stable in aqueous solution containing 1% DMF or 1% DMSO for at least 3 h. After 6 h, however, the nitro-NHC ligand was released to a significant degree and might provide a route of decomposition. In contrast, the COD ligand remained largely coordinated throughout the incubation period, although the mass signal at *m/z* 509.97 was indicative of some COD release. The mass spectra of the DMSO and DMF solutions were very similar, featuring several selective and nonselective solvent adducts with the organometallics. Compound **2c** eventually forms a dimeric compound corresponding to [Rh₂(COD)₂(μ -Cl)₃(OH)₂ – 2H][–], whereas unambiguous decomposition products of **2d** are still elusive.

Of note, in a previous study, we observed rapid cellular uptake of the structurally related complex Rh(I)(NHC)(COD)Cl (see [Figure 1](#)) within 1–4 h.¹⁷ Accordingly, it can be speculated that the complexes reach the cellular environment in an intact form and that the mentioned ligand-exchange processes occur mainly inside the cells, leading to bioactive metabolites. Importantly, the observed products of hydrolysis are of a cationic nature, and this indicates some analogies with the biochemistry of cisplatin, which forms cationic aqua complexes upon intracellular hydrolysis that represent the species attacking DNA.³⁷ Also regarding cellular metabolism, interactions with molecular targets have to be considered (e.g., glutathione or other cellular thiols).

The above-noted differences between the iodido and chlorido ligands also were reflected in certain differences in their biological activities. Whereas the chlorido derivative **2c** was a stronger uncoupling-like agent in mitochondria, the iodido complex **2d** triggered stronger activity against general cellular metabolism (impedance, respiration, acidification; see the [Supporting Information](#) for details). However, the observed activities required rather high concentrations and can therefore be considered as secondary effects.

Clear effects at lower concentrations were observed on cellular signaling determined by ELISA microarrays that had previously been developed to study the activation of major pathways controlling stress response and cellular proliferation.^{38,39} In these experiments, the two complexes triggered comparably strong phosphorylations of HSP27, and MAPKs such as p38 and ERK1/2 were also significantly activated, reflecting a general cellular stress response. In the case of MAPK phosphorylation, the chlorido complex **2c** showed

higher efficiency. Other important signaling targets that were modulated included FAK and p70S6.

The observed phosphorylation profiles differ significantly from results obtained for cisplatin and camptothecin, which directly target DNA or replication. In comparable assays, although under slightly different conditions and with another cancer cell line in the case of cisplatin, these compounds did not lead to ERK1/2 phosphorylation.⁴⁰ Within 8–11 h, cisplatin also did not affect Akt1 and GSK-3 β phosphorylation levels but showed a decrease after 24 h.⁴⁰ Complexes **2c** and **2d** initially decreased GSK-3 β phosphorylation, but levels increased after longer incubation. Akt1 was not strongly influenced by **2c** and **2d** (small decrease of phosphorylation). These results indicate that the mode of action of rhodium(I) NHC complexes differs significantly from the activities of cisplatin or camptothecin. This is further confirmed by the only weak activation of Chk2 that is activated in response to DNA damage and replication stress.³⁸ Regarding a comparison with recently studied gold species, complexes **2c** and **2d** showed a pattern similar to that of previously studied phosphane-containing complexes (e.g., auranofin) that also triggered ERK, p38, and HSP27 activation but differing from that of a biscarbene gold complex, which, again, did not activate ERK phosphorylation.^{41,42}

Screening of an extended series of Rh(I)(NHC)(COD)X complexes for their antiproliferative effects against two cancer lines showed, in general, a certain preference for iodido over chlorido ligands. However, the couple **2c/2d** represented an exception where no clear trend could be noted in this respect. Advantages of switching from chlorido to iodido complexes were previously reported by Sadler and co-workers for organometallic complexes of the type [M(*p*-cymene)(azo/imino-pyridine)X]⁺, where M was Ru or Os and X was Cl or I.⁴³ In that case, the iodido complexes were also more potent and differed in other anticancer-related properties such as p53 dependency for activity.

Further conclusions regarding structure–activity relationships for cytotoxicity indicated a preference for the methyl group (see results for **3c/d** in Table 1), which exhibits a positive inductive effect that might enhance the donor capacity of the NHC ligand, or the unsubstituted NHC ligand, which afforded higher cytotoxicity in our previous study.¹⁷ Taken together, future lead-optimization strategies for Rh(I) NHC complexes should further address the coordinated halide ligands as well as the fine-tuning of donor properties of the NHC ligand system. Regarding our previous report, solubility plays a deciding role, and therefore, rather low-lipophilicity NHC ligands should be preferred in future studies. Replacement of the chlorido ligand with CO has already been investigated, but it turned out to be problematic in terms of lipophilicity and stability in solution.¹⁷

In summary, our study shows that the biological properties of rhodium(I) NHC complexes can be modulated by changing the substituents on the NHC ligands and the nature of the secondary halide ligand. Regarding their mode of drug action, effects on cellular signaling of certain targets such as p38, ERK1, and ERK2 have to be taken into account.

Taken together with previous reports,^{8,9,15–17} this study shows that the Rh(I)(NHC)(COD) fragment might represent a useful organometallic pharmacophore for the design of novel anticancer and antibacterial agents that interfere with MAPK signaling and other yet-to-be-identified targets.

EXPERIMENTAL SECTION

General. All reagents and solvents were used as received from Sigma, Aldrich, or Acros. 5-Methoxybenzimidazole (**4a**) was obtained from Acros. ¹H NMR and ¹³C NMR spectra were recorded on a Bruker DRX-400 AS NMR System; MS spectra were recorded on a FinniganMAT4515. The purities of the target compounds (>95%) were confirmed by elemental analysis (Flash EA112, Thermo Quest Italia). For all compounds undergoing biological evaluation, the experimental values differed by less than 0.5% from the calculated ones.

5-Chlorobenzimidazole (1a).⁴⁴ 4-Chloro-1,2-phenyldiamine (1.891 g, 13.26 mmol) and 40 mL of formic acid were added to a 100 mL flask and refluxed at 110 °C for 4 h, giving a deep blue solution. The mixture was cooled to 0 °C, and the product was precipitated by neutralization with concentrated ammonia. **1a** was filtered off, washed twice with water, and dried at 50 °C. Yield: 1.911 g (12.53 mmol, 95%), purple powder. ¹H NMR (CDCl₃, ppm): 10.43 (s, 1H, NH), 8.20 (s, 1H, ArH2), 7.65 (d, 1H, ⁴J = 2.0 Hz, ArH4), 7.55 (d, 1H, ³J = 8.8 Hz, ArH7), 7.27 (dd, 1H, ⁴J = 2.0 Hz, ³J = 8.8 Hz, ArH6). ¹³C NMR (CDCl₃): 141.3 (ArC-2), 138.2 (ArC-Cl), 136.3 (ArC-7a), 128.8 (ArC-3a), 123.7 (ArC-6), 116.4 (ArC-4), 115.4 (ArC-7). Elemental analysis for C₇H₅ClN₂ (% calcd/found): C (55.10/54.20), H (3.30/3.30), N (18.36/17.87).

5-Nitrobenzimidazole (2a).⁴⁴ 4-Nitro-1,2-phenyldiamine (1.784 g, 11.65 mmol) and 40 mL of formic acid were added to a 100 mL flask and refluxed at 110 °C for 4 h, giving a green solution. The mixture was cooled to 0 °C, and the product was precipitated by neutralization with concentrated ammonia. **2a** was filtered off, washed twice with water, and dried at 50 °C. Yield: 1.621 g (9.94 mmol, 85%), light green powder. ¹H NMR (DMSO-*d*₆, ppm): 13.10 (s, 1H, NH), 8.56 (s, 1H, ArH2), 8.52 (dd, 1H, ⁵J = 0.5 Hz, ⁴J = 2.3 Hz, ArH4), 8.15 (dd, 1H, ⁴J = 2.3 Hz, ³J = 8.8 Hz, ArH6), 7.77 (dd, 1H, ⁵J = 0.5 Hz, ³J = 8.8 Hz, ArH7). ¹³C NMR (DMSO-*d*₆): 146.8 (ArC-2), 142.6 (ArC-NO₂), 117.6 (ArC-6), 114.9 (ArC-4), 112.8 (ArC-7). Elemental analysis for C₇H₅O₂N₃ (% calcd/found): C (51.54/51.48), H (3.09/2.97), N (25.76/25.65).

5-Methylbenzimidazole (3a).⁴⁵ 4-Methyl-1,2-phenyldiamine (0.579 g, 4.74 mmol) and 20 mL of formic acid were added to a 100 mL flask and refluxed at 110 °C for 4 h, giving a red-brown solution. The mixture was cooled to 0 °C and neutralized with concentrated ammonia, and the solvent was removed under reduced pressure. **3a** was extracted with dichloromethane, which was removed by reduced pressure. The product was highly hygroscopic brown oil. Yield: 0.510 g (3.86 mmol, 81%), brown oil. ¹H NMR (CDCl₃, ppm): 12.73 (s, 1H, NH), 8.26 (s, 1H, ArH2), 7.54 (d, 1H, ³J = 8.3 Hz, ArH7), 7.44 (s, 1H, ArH4), 7.13 (d, 1H, ³J = 8.3, ArH6), 2.4 (s, 3H, -CH₃). ¹³C NMR (CDCl₃): 139.7 (ArC-2), 135.6 (ArC-CH₃), 134.1 (ArC-3a), 133.9 (ArC-7a), 125.4 (ArC-7), 114.8 (ArC-4), 114.5 (ArC-6), 21.5 (-CH₃). Elemental analysis for C₈H₈N₂ (% calcd/found): C (72.70/69.78), H (6.10/5.95), N (21.20/19.84).

General Procedure for Synthesis of the Benzimidazolium Iodides 1b–4b. One equivalent of substituted benzimidazole, 1 equiv of K₂CO₃, and an excess of methyl iodide were heated under reflux in acetonitrile/toluene (1:1) for 12 h. The solvent was removed under reduced pressure, and the resultant solid was resuspended in dichloromethane and filtered to remove the formed potassium iodide along with the remaining K₂CO₃. The solvent of the filtrate was removed under reduced pressure, and the product resuspended in tetrahydrofuran to remove the excess methyl iodide and unreacted substituted benzimidazole.

5-Chloro-1,3-dimethylbenzimidazolium iodide (1b). **1a** (0.391 g, 2.56 mmol), K₂CO₃ (0.354 g, 2.56 mmol) and methyl iodide (0.7 mL, 10.25 mmol) were dissolved in 20 mL of acetonitrile/toluene (1:1) and refluxed for 12 h. Yield: 0.354 g (1.95 mmol, 76%), purple powder. ¹H NMR (CDCl₃, ppm): 9.69 (s, 1H, ArH2), 8.28 (d, 1H, ⁴J = 2.0 Hz, ArH4), 8.06 (d, 1H, ³J = 8.8 Hz, ArH7), 7.78 (dd, 1H, ⁴J = 2.0 Hz, ³J = 8.8 Hz, ArH6), 4.08 (s, 3H, N-CH₃), 3.98 (s, 3H, N-CH₃). ¹³C NMR (CDCl₃): 156.2 (ArC-Cl), 144.3 (ArC-2), 132.5 (ArC-7a), 131.1 (ArC-3a), 126.7 (ArC-6), 115.1 (ArC-4), 113.7 (ArC-

7), 34.3 (N-CH₃), 34.1 (N-CH₃). Elemental analysis for C₉H₁₀ClN₂I (% calcd/found): C (35.03/36.45), H (3.27/3.39), N (9.08/8.50)

1,3-Dimethyl-5-nitrobenzimidazolium Iodide (2b). **2a** (0.313 g, 1.92 mmol), K₂CO₃ (0.300 g, 1.92 mmol), and methyl iodide (0.5 mL, 7.67 mmol) were dissolved in 20 mL of acetonitrile/toluene (1:1) and refluxed for 12 h. Yield: 0.338 g (1.75 mmol, 91%), light brown powder. ¹H NMR (DMSO-*d*₆, ppm): 9.94 (s, 1H, ArH2), 9.08 (dd, 1H, ⁵J = 0.5 Hz, ⁴J = 2.3 Hz, ArH4), 8.57 (dd, 1H, ⁴J = 2.3 Hz, ³J = 9.0 Hz, ArH6), 8.27 (dd, 1H, ⁵J = 0.5 Hz, ³J = 9.0 Hz, ArH7), 4.19 (s, 3H, N-CH₃), 4.15 (s, 3H, N-CH₃). ¹³C NMR (DMSO-*d*₆): 147.4 (ArC-2), 145.5 (ArC-NO₂), 135.3 (ArC-7a), 131.5 (ArC-3a), 121.4 (ArC-6), 114.8 (ArC-4), 110.8 (ArC-7), 33.8 (2× N-CH₃). Elemental analysis for C₉H₁₀O₂N₃I (% calcd/found): C (33.88/33.97), H (3.16/3.27), N (13.17/11.94).

1,3,5-Trimethylbenzimidazolium Iodide (3b). **3a** (0.510 g, 3.86 mmol), K₂CO₃ (0.540 g, 3.86 mmol), and methyl iodide (1.0 mL, 15.44 mmol) were dissolved in 20 mL of acetonitrile/toluene (1:1) and refluxed for 12 h. Yield: 0.611 g (2.12 mmol, 54.9%), white powder. ¹H NMR (CDCl₃, ppm): 11.03 (s, 1H, ArH2), 7.57 (d, 1H, ³J = 8.6 Hz, ArH7), 7.51 (dd, 1H, ⁴J = 1.0 Hz, ³J = 8.6 Hz, ArH6), 7.48 (d, 1H, ⁴J = 1.0 Hz, ArH4), 4.24 (s, 3H, N-CH₃), 4.23 (s, 3H, N-CH₃), 2.61 (s, 3H, -CH₃). ¹³C NMR (CDCl₃): 142.3 (ArC-2), 138.5 (ArC-CH₃), 132.1 (ArC-3a), 130.0 (ArC-7a), 129.1 (ArC-7), 112.2 (ArC-6), 112.2 (ArC-4), 33.8 (N-CH₃), 33.7 (N-CH₃), 21.9 (-CH₃). Elemental analysis for C₁₀H₁₃N₃I (% calcd/found): C (41.69/41.46), H (4.55/4.50), N (9.72/9.72).

5-Methoxy-1,3-dimethylbenzimidazolium Iodide (4b). 5-Methoxybenzimidazole (0.706 g, 4.77 mmol), K₂CO₃ (0.700 g, 4.77 mmol), and methyl iodide (1.2 mL, 19.06 mmol) were dissolved in 20 mL of acetonitrile/toluene (1:1) and refluxed for 12 h. Yield: 0.944 g (3.10 mmol, 65%), brown powder. ¹H NMR (CDCl₃, ppm): 10.73 (s, 1H, ArH2), 7.58 (dd, 1H, ⁴J = 1.6 Hz, ³J = 7.8 Hz, ArH7), 7.21 (dd, 1H, ⁴J = 2.3 Hz, ³J = 7.8 Hz, ArH6), 7.16 (d, 1H, ⁴J = 2.3 Hz, ArH4), 4.22 (s, 3H, N-CH₃), 4.19 (s, 3H, N-CH₃), 3.95 (s, 3H, -OCH₃). ¹³C NMR (CDCl₃): 159.5 (ArC-OCH₃), 153.8 (ArC-2), 141.6 (ArC-3a), 132.8 (ArC-7a), 116.9 (ArC-7), 113.3 (ArC-4), 95.5 (ArC-6), 56.8 (-OCH₃), 33.4 (N-CH₃), 33.1 (N-CH₃). Elemental analysis for C₁₀H₁₃ON₂I (% calcd/found): C (39.49/40.26), H (4.31/4.31), N (9.21/9.04).

General Procedure for Synthesis of Rhodium NHC Complexes 1c/d–4c/d. One equivalent of the respective benzimidazolium iodide **1b–4b** and 0.5 equiv of Ag₂O were added to a dried Schlenk tube. The mixture was back-flashed three times with N₂, and then 15 mL of dry CH₂Cl₂ were added. The flask was closed, and the mixture was stirred for 4 h in the dark. A solution containing 0.5 equiv of bis[halido(η²,η²-cycloocta-1,5-diene)rhodium(I)] in CH₂Cl₂ was added (10 mL), and the solution was stirred for 2 h in the dark. The obtained suspension was filtered over Celite (281 nm) and concentrated in a vacuum. The yellow residue was recrystallized from CH₂Cl₂/*n*-hexane (10 mL/40 mL) at 4 °C.

Chlorido(5-chloro-1,3-dimethylbenzimidazol-2-ylidene)(η²,η²-cycloocta-1,5-diene)rhodium(I) (1c). **1b** (0.096 g, 0.31 mmol), Ag₂O (0.042 g, 0.18 mmol), bis[chlorido(η²,η²-cycloocta-1,5-diene)rhodium(I)] (0.078 g, 0.14 mmol), 2 h. Yield: 0.054 g (0.13 mmol, 41%), yellow powder. ¹H NMR (CDCl₃, ppm): 7.28 (dd, 1H, ⁵J = 0.5 Hz, ⁴J = 1.7 Hz, ArH4), 7.21 (dd, 1H, ⁴J = 1.7 Hz, ³J = 8.5 Hz, ArH6), 7.18 (dd, 1H, ⁵J = 0.5 Hz, ³J = 8.5 Hz, ArH7), 5.17 (s, 2H, CH-COD), 4.29 (s, 3H, N-CH₃), 4.28 (s, 3H, N-CH₃), 3.36 (s, 2H, CH-COD), 2.47 (m, 4H, CH₂-COD), 2.02 (m, 4H, CH₂-COD). ¹³C NMR (CDCl₃): 198.3 (d, ¹J = 50.9 Hz, ArC-2), 135.9 (ArC-Cl), 134.0 (ArC-7a), 128.7 (ArC-3a), 122.7 (ArC-6), 109.9 (ArC-4), 109.6 (ArC-7), 100.8 (d, ¹J = 6.6 Hz, CH-COD), 100.7 (d, ¹J = 6.6 Hz, CH-COD), 68.5 (d, ¹J = 14.6 Hz, CH-COD), 68.4 (d, ¹J = 14.6 Hz, CH-COD), 34.8 (s, N-CH₃), 34.8 (s, N-CH₃), 32.9 (CH₂-COD), 32.9 (CH₂-COD), 28.8 (CH₂-COD), 28.8 (CH₂-COD); MS(EI): 426 (M⁺). Elemental analysis for C₁₇H₂₁N₂Cl₂Rh (% calcd/found): C (47.80/47.93), H (4.96/5.55), N (6.56/5.05).

(5-Chloro-1,3-dimethylbenzimidazol-2-ylidene)(η²,η²-cycloocta-1,5-diene)iodidorhodium(I) (1d). **1b** (0.093 g, 0.31 mmol), Ag₂O

(0.042 g, 0.18 mmol), bis[iodido(η²,η²-cycloocta-1,5-diene)rhodium(I)] (0.085 g, 0.12 mmol), 2 h. Yield: 0.044 g (0.09 mmol, 28%), light brown powder. ¹H NMR (CDCl₃, ppm): 7.28 (dd, 1H, ⁵J = 0.6 Hz, ⁴J = 1.7 Hz, ArH4), 7.20 (dd, 1H, ⁴J = 1.7 Hz, ³J = 8.5 Hz, ArH6), 7.18 (dd, 1H, ⁵J = 0.6 Hz, ³J = 8.5 Hz, ArH7), 5.37 (s, 2H, CH-COD), 4.18 (s, 3H, N-CH₃), 4.17 (s, 3H, N-CH₃), 3.52 (s, 2H, CH-COD), 2.38 (m, 4H, CH₂-COD), 2.05 (m, 2H, CH₂-COD), 1.88 (m, 2H, CH₂-COD). ¹³C NMR (CDCl₃): 198.9 (d, ¹J = 49.5 Hz, NHC), 136.1 (ArC-Cl), 134.2 (ArC-7a), 128.5 (ArC-3a), 122.5 (ArC-4), 109.8 (ArC-6), 109.5 (ArC-7), 98.6 (d, ¹J = 5.2 Hz, CH-COD), 98.5 (d, ¹J = 5.2 Hz, CH-COD), 71.9 (d, ¹J = 14.0 Hz, CH-COD), 71.8 (d, ¹J = 14.0 Hz, CH-COD), 34.9 (N-CH₃), 34.8 (N-CH₃), 32.3 (CH₂-COD), 32.3 (CH₂-COD), 29.5 (CH₂-COD), 29.5 (CH₂-COD); MS(EI): 518 (M⁺). Elemental analysis for C₁₇H₂₁N₂ClIRh (% calcd/found): C (39.37/40.67), H (4.08/4.05), N (5.40/5.25).

Chlorido(η²,η²-cycloocta-1,5-diene)(5-nitro-1,3-dimethylbenzimidazol-2-ylidene)rhodium(I) (2c). **2b** (0.102 g, 0.32 mmol), Ag₂O (0.044 g, 0.19 mmol), bis[chlorido(η²,η²-cycloocta-1,5-diene)rhodium(I)] (0.089 g, 0.16 mmol), 2 h. Yield: 0.117 g (0.27 mmol, 84%), yellow powder. ¹H NMR (CDCl₃, ppm): 8.24 (dd, 1H, ⁴J = 2.1 Hz, ³J = 8.6 Hz, ArH6), 8.22 (d, 1H, ⁴J = 2.1 Hz, ArH4), 7.35 (d, 1H, ³J = 8.6 Hz, ArH7), 5.24 (s, 2H, CH-COD), 4.40 (s, 3H, N-CH₃), 4.39 (s, 3H, N-CH₃), 3.40 (s, 2H, CH-COD), 2.50 (m, 4H, CH₂-COD), 2.09 (m, 4H, CH₂-COD). ¹³C NMR (CDCl₃): 204.5 (d, ¹J = 51.0 Hz, NHC), 143.4 (ArC-NO₂), 138.7 (ArC-7a), 134.9 (ArC-3a), 118.7 (ArC-6), 109.0 (ArC-4), 105.5 (ArC-7), 101.9 (d, ¹J = 6.5 Hz, CH-COD), 101.8 (d, ¹J = 6.5 Hz, CH-COD), 68.9 (d, ¹J = 14.2 Hz, CH-COD), 68.8 (d, ¹J = 14.2 Hz, CH-COD), 35.2 (N-CH₃), 35.2 (N-CH₃), 33.0 (CH₂-COD), 33.0 (CH₂-COD), 28.8 (CH₂-COD), 28.8 (CH₂-COD); MS(EI): 437 (M⁺). Elemental analysis for C₁₇H₂₁O₂N₃ClIRh (% calcd/found): C (46.65/46.85), H (4.84/5.04), N (9.60/8.05).

(η²,η²-Cycloocta-1,5-diene)iodido(5-nitro-1,3-dimethylbenzimidazol-2-ylidene)rhodium(I) (2d). **2b** (0.091 g, 0.29 mmol), Ag₂O (0.025 g, 0.10 mmol), bis[iodido(η²,η²-cycloocta-1,5-diene)rhodium(I)] (0.050 g, 0.07 mmol), 2 h. Yield: 0.044 g (0.011 mmol, 38%), light brown powder. ¹H NMR (CDCl₃, ppm): 8.23 (dd, 1H, ⁵J = 0.6 Hz, ⁴J = 2.1 Hz, ArH4), 8.21 (dd, 1H, ⁴J = 2.1 Hz, ³J = 8.5 Hz, ArH6), 7.36 (dd, 1H, ⁵J = 0.6 Hz, ³J = 8.5 Hz, ArH7), 5.42 (s, 2H, CH-COD), 4.29 (s, 3H, N-CH₃), 4.28 (s, 3H, N-CH₃), 3.56 (s, 2H, CH-COD), 2.42 (m, 4H, CH₂-COD), 2.14 (m, 2H, CH₂-COD), 1.91 (m, 2H, CH₂-COD). ¹³C NMR (CDCl₃): 205.3 (d, ¹J = 48.6 Hz, NHC), 143.2 (ArC-NO₂), 138.2 (ArC-7a), 135.1 (ArC-3a), 118.7 (ArC-6), 108.8 (ArC-4), 105.3 (ArC-7), 99.6 (d, ¹J = 6.2 Hz, CH-COD), 99.5 (d, ¹J = 6.2 Hz, CH-COD), 72.3 (d, ¹J = 14.2 Hz, CH-COD), 72.2 (d, ¹J = 14.2 Hz, CH-COD), 35.3 (N-CH₃), 35.2 (N-CH₃), 32.3 (CH₂-COD), 32.3 (CH₂-COD), 29.4 (CH₂-COD), 29.4 (CH₂-COD); MS(EI): 529 (M⁺). Elemental analysis for C₁₇H₂₁O₂N₃IRh (% calcd/found): C (38.58/39.06), H (4.00/4.10), N (7.94/7.78).

Chlorido(η²,η²-cycloocta-1,5-diene)(1,3,5-trimethylbenzimidazol-2-ylidene)rhodium(I) (3c). **3b** (0.092 g, 0.32 mmol), Ag₂O (0.053 g, 0.23 mmol), bis[chlorido(η²,η²-cycloocta-1,5-diene)rhodium(I)] (0.082 g, 0.15 mmol), 2 h. Yield: 0.082 g (0.20 mmol, 63%), yellow powder. ¹H NMR (CDCl₃, ppm): 7.14 (d, 1H, ³J = 8.2 Hz, ArH7), 7.07 (t, 1H, ⁵J = 0.8 Hz, ArH4), 7.03 (ddd, 1H, ⁵J = 0.8 Hz, ³J = 8.2 Hz, ArH6), 5.15 (s, 2H, CH-COD), 4.27 (s, 3H, N-CH₃), 4.26 (s, 3H, N-CH₃), 3.35 (s, 2H, CH-COD), 2.46 (m, 4H, CH₂-COD), 2.46 (s, 3H, CH₃), 2.01 (m, 4H, CH₂-COD). ¹³C NMR (CDCl₃): 195.2 (d, ¹J = 50.6 Hz, ArC-2), 135.6 (ArC-CH₃), 133.5 (ArC-3a), 132.5 (ArC-7a), 123.8 (ArC-7), 109.5 (ArC-4), 108.8 (ArC-6), 100.1 (d, ¹J = 2.3 Hz, CH-COD), 100.0 (d, ¹J = 2.3 Hz, CH-COD), 68.3 (d, ¹J = 14.5 Hz, CH-COD), 68.2 (d, ¹J = 14.5 Hz, CH-COD), 34.6 (N-CH₃), 34.5 (N-CH₃), 32.9 (CH₂-COD), 32.9 (CH₂-COD), 28.9 (CH₂-COD), 28.9 (CH₂-COD), 21.8 (-CH₃); MS(EI): 406 (M⁺). Elemental analysis for C₁₈H₂₄N₂ClIRh (% calcd/found): C (53.15/53.11), H (5.95/5.87), N (6.89/6.53).

(η²,η²-Cycloocta-1,5-diene)iodido(1,3,5-trimethylbenzimidazol-2-ylidene)rhodium(I) (3d). **3b** (0.077 g, 0.27 mmol), Ag₂O (0.029 g, 0.13 mmol), bis[iodido(η²,η²-cycloocta-1,5-diene)rhodium(I)] (0.098

g, 0.13 mmol). Yield: 0.012 g (0.02 mmol, 9%), light brown powder. ^1H NMR (CDCl_3 , ppm): 7.13 (d, 1H, $^3J = 8.2$ Hz, ArH7), 7.07 (t, 1H, $^5J = 0.9$ Hz, ArH4), 7.04 (dd, 1H, $^5J = 0.9$ Hz, $^3J = 8.2$, ArH6), 5.32 (s, 2H, CH-COD), 4.16 (s, 6H, N-CH₃), 3.51 (s, 2H, CH-COD), 2.46 (s, 3H, -CH₃), 2.37 (m, 4H, CH₂-COD), 2.03 (m, 2H, CH₂-COD), 1.85 (m, 2H, CH₂-COD). ^{13}C NMR (CDCl_3): 192.4 (d, $^1J = 53.6$ Hz, NHC), 135.3 (ArC-CH₃), 133.6 (ArC-3a), 133.2 (ArC-7a), 124.4 (ArC-7), 109.9 (ArC-4), 109.4 (ArC-6), 91.2 (d, $^1J = 7.2$ Hz, CH-COD), 91.1 (d, $^1J = 7.2$ Hz, CH-COD), 35.9 (d, $^1J = 15.4$ Hz, CH-COD), 35.8 (d, $^1J = 15.4$ Hz, CH-COD), 33.8 (N-CH₃), 33.8 (N-CH₃), 30.8 (CH₂-COD), 30.8 (CH₂-COD), 30.7 (CH₂-COD), 30.7 (CH₂-COD), 21.4 (-CH₃); MS(EI): 498 (M^+). Elemental analysis for $\text{C}_{18}\text{H}_{23}\text{N}_2\text{Irh}$ (% calcd/found): C (43.39/43.69), H (4.86/4.70), N (5.62/4.98).

Chlorido(η^2,η^2 -cycloocta-1,5-diene)(1,3-dimethyl-5-methoxybenzimidazol-2-ylidene)rhodium(I) (4c). **4b** (0.085 g, 0.28 mmol), Ag_2O (0.050 g, 0.21 mmol), bis[chlorido(η^2,η^2 -cycloocta-1,5-diene)rhodium(I)] (0.079 g, 0.14 mmol). Yield: 0.030 g (0.07 mmol, 25%), yellow powder. ^1H NMR (CDCl_3 , ppm): 7.15 (d, 1H, $^3J = 8.7$ Hz, ArH7), 6.83 (dd, 1H, $^4J = 2.3$ Hz, $^3J = 8.7$ Hz, ArH6), 6.75 (d, 1H, $^4J = 2.3$ Hz, ArH4), 5.14 (s, 2H, CH-COD), 4.26 (s, 6H, N-CH₃), 3.85 (s, 3H, -OCH₃), 3.35 (s, 2H, CH-COD), 2.46 (m, 4H, CH₂-COD), 2.01 (m, 4H, CH₂-COD). ^{13}C NMR (CDCl_3): 195.3 (d, $^1J = 50.6$ Hz, NHC), 156.4 (ArC-OCH₃), 136.1 (ArC-3a), 130.0 (ArC-7a), 110.3 (ArC-7), 109.7 (ArC-6), 100.0 (d, $^1J = 6.5$ Hz, CH-COD), 94.0 (ArC-4) 68.3 (d, $^1J = 14.5$ Hz, CH-COD), 68.2 (d, $^1J = 14.5$ Hz, CH-COD), 56.0 (-OCH₃), 35.0 (N-CH₃), 35.0 (N-CH₃), 32.9 (CH₂-COD), 32.9 (CH₂-COD), 28.4 (CH₂-COD); MS(EI): 422 (M^+). Elemental analysis for $\text{C}_{18}\text{H}_{24}\text{ON}_2\text{ClRh}$ (% calcd/found): C (51.14/51.54), H (5.72/5.63), N (6.63/6.56).

(η^2,η^2 -Cycloocta-1,5-diene)iodido(1,3-dimethyl-5-methoxybenzimidazol-2-ylidene)rhodium(I) (4d). **4b** (0.079 g, 0.26 mmol), Ag_2O (0.047 g, 0.20 mmol), bis[iodido(η^2,η^2 -cycloocta-1,5-diene)rhodium(I)] (0.095 g, 0.13 mmol). Yield: 0.032 g (0.06 mmol, 24%), light brown powder. ^1H NMR (CDCl_3 , ppm): 7.13 (d, 1H, $^3J = 8.2$ Hz, ArH7), 6.82 (dd, 1H, $^4J = 3.0$ Hz, $^3J = 8.2$ Hz, ArH6), 6.76 (d, 1H, $^4J = 3.0$ Hz, ArH4), 5.32 (s, 2H, CH-COD), 4.16 (s, 6H, N-CH₃), 3.85 (s, 3H, -OCH₃), 3.52 (s, 2H, CH-COD), 2.37 (m, 4H, CH₂-COD), 2.04 (m, 2H, CH₂-COD), 1.86 (m, 2H, CH₂-COD). ^{13}C NMR (CDCl_3): 175.5 (d, $^1J = 48.3$ Hz, NHC), 156.3 (ArC-OCH₃), 136.3 (ArC-3a), 130.3 (ArC-7a), 110.1 (ArC-7), 109.6 (ArC-4), 97.9 (d, $^1J = 6.3$ Hz, CH-COD), 94.0 (ArC-6), 71.7 (d, $^1J = 14.1$ Hz, CH-COD), 71.7 (d, $^1J = 14.1$ Hz, CH-COD), 56.0 (-OCH₃), 35.9 (N-CH₃), 35.6 (N-CH₃), 30.8 (CH₂-COD), 30.8 (CH₂-COD), 27.2 (CH₂-COD); MS(EI): 514 (M^+). Elemental analysis for $\text{C}_{18}\text{H}_{24}\text{ON}_2\text{Irh}$ (% calcd/found): C (42.02/42.25), H (4.70/4.79), N (5.45/4.95).

Mass Spectrometry. The compounds were dissolved at 10 mM in dimethyl sulfoxide (DMSO, Sigma) and *N,N*-dimethylformamide (DMF, Acros), and the solutions were diluted with unbuffered water (MilliPore) to 100 μM and incubated in the dark at 37 °C. ESI mass spectra in positive- and negative-ion modes were recorded after 10, 60, 120, 180, and 360 min and after 24 h. Aliquots were then further diluted to 5–10 μM prior to injection into the mass spectrometer. Mass spectra were recorded on a Bruker AmaZon SL electrospray ionization ion-trap (ESI-IT) mass spectrometer, and the resulting data files were processed using Bruker Compass 1.3 and DataAnalysis 4.0. The compounds were injected by direct infusion into the mass spectrometer at 5 $\mu\text{L}/\text{min}$, and typical experimental conditions were as follows: ± 4.5 kV capillary voltage, 63% RF level, 55.2 trap drive, 180 °C dry temperature, 8 psi nebulizer, 6 L/min dry gas. The average accumulation time in positive-ion mode was approximately 1 ms. Experimental mass signals include a standard deviation of $m/z \pm 0.02$.

Cell Culture, Time-Course Experiments, and Lysate Preparation for Microarray ELISA. Colon cancer cell line HT-29 (ATCC) was maintained in DMEM High Glucose containing 10% fetal calf serum (both from PAA Laboratories) at 37 °C with 5% CO_2 . Cells were seeded in six-well plates (35 mm) at a density of 3×10^5 cells/well and were grown for 24 h under standard cell culture conditions to 60–70% confluence. For treatment, a stock solution of **2c** or **2d** in dimethylformamide (DMF) was freshly prepared and

added to cells without medium replacement (final DMF concentration = 0.1% v/v). For mock treatment, cells were incubated with 0.1% (v/v) DMF only. At indicated time points, cells were washed three times with ice-cold D-PBS (Invitrogen) and lysed in 100 μL lysis buffer (6 M urea, 1 mM EDTA, 0.5% Triton X-100, 5 mM NaF, 10 $\mu\text{g}/\text{mL}$ leupeptin, 10 $\mu\text{g}/\text{mL}$ pepstatin, 100 μM PMSF, 3 $\mu\text{g}/\text{mL}$ aprotinin, 2.5 mM $\text{Na}_4\text{P}_2\text{O}_7$, 1 mM Na_3VO_4 in D-PBS). Collected samples were centrifuged for 15 min at 4 °C and 13,000 rpm, and supernatants were frozen at –80 °C for further analysis.

Total Protein Concentration. Total protein concentration was determined using the BCA Protein Assay (Pierce Biotechnology) in a 96-well-plate format.

ELISA Microarray Protocol. Proteins were quantified using sandwich ELISA microarrays. The microarrays were based on the ArrayStripTM platform (Alere Technologies GmbH). A detailed description of the assay protocol, information on the reagents for this assay, and a list of the currently available targets were previously reported.³⁹ In brief, cellular samples were diluted 1:6 with dilution buffer (1 mM EDTA, 0.5% Triton X-100, 5 mM sodium fluoride, 1 M urea in buffered saline, pH 7.2) and incubated with microarrays for 60 min. A detection cocktail of 15 biotin-labeled phospho-specific detection antibodies (R&D Systems) was used, with the concentration of each antibody at 18 ng/mL. Colorimetric signals were detected by transmission measurements with the ArraymateTM reader (Alere Technology GmbH). Kinetic microarray data were analyzed with KOMA software.³⁰ Total protein concentrations were used for signal normalization. The final results were calculated from two independent experiments and are expressed as mean values with errors (standard error of the mean, SEM).

Antiproliferative Effects in HT-29 and MDA-MB-231 Cells. MCF-7 breast adenocarcinoma and HT-29 colon carcinoma cells were maintained in DMEM High Glucose (PAA) supplemented with 50 mg/L gentamycin and 10% (v/v) fetal calf serum (FCS) prior to use. The antiproliferative effects of the compounds were determined by the crystal violet assay following an established procedure that was applied in a number of previous studies.^{47–50} The results were calculated as IC_{50} values obtained from two to three independent experiments and are expressed as mean values \pm SEM.

■ ASSOCIATED CONTENT

📄 Supporting Information

The Supporting Information is available free of charge on the ACS Publications website at DOI: 10.1021/acs.jmedchem.5b01159.

More details on mass spectrometry, effects on mitochondria and cell metabolism, additional ELISA array data (PDF)

■ AUTHOR INFORMATION

Corresponding Author

*E-mail: ingo.ott@tu-bs.de. Tel.: +49 531 3912743.

Notes

The authors declare no competing financial interest.

■ ACKNOWLEDGMENTS

The support by COST action CM1105 (Functional metal complexes that bind to biomolecules) and the technical assistance of Filip Groznica for performing some of the ESI-MS measurements are gratefully acknowledged.

■ ABBREVIATIONS USED

BCA, bicinchoninic acid; COD, η^2,η^2 -cycloocta-1,5-diene; CREB, cAMP response element-binding protein; ERK, extracellular-signal-regulated kinase; FCS, fetal calf serum;

FAK, focal adhesion kinase; HSP, heat-shock protein; NHC, N-heterocyclic carbene

REFERENCES

- (1) Hartinger, C. G.; Metzler-Nolte, N.; Dyson, P. J. Challenges and opportunities in the development of organometallic anticancer drugs. *Organometallics* **2012**, *31*, 5677–5685.
- (2) Gasser, G.; Ott, I.; Metzler-Nolte, N. Organometallic anticancer compounds. *J. Med. Chem.* **2011**, *54*, 3–25.
- (3) Noffke, A. L.; Habtemariam, A.; Pizarro, A. M.; Sadler, P. J. Designing organometallic compounds for catalysis and therapy. *Chem. Commun.* **2012**, *48*, 5219–5246.
- (4) Oehninger, L.; Rubbiani, R.; Ott, I. N-Heterocyclic carbene metal complexes in medicinal chemistry. *Dalton Trans.* **2013**, *42*, 3269–3284.
- (5) Kascatan-Nebioglu, A.; Panzner, M. J.; Tessier, C. A.; Cannon, C. L.; Youngs, W. J. N-Heterocyclic carbene–silver complexes: A new class of antibiotics. *Coord. Chem. Rev.* **2007**, *251*, 884–895.
- (6) Cisnetti, F.; Gautier, A. Metal/N-heterocyclic carbene complexes: Opportunities for the development of anticancer metallodrugs. *Angew. Chem., Int. Ed.* **2013**, *52*, 11976–11978.
- (7) Cetinkaya, B.; Özdemir, I.; Binbaşıoğlu, B.; Durmaz, R.; Günel, S. Antibacterial and antifungal activities of complexes of ruthenium(II). *Arzneim. Forsch.* **1999**, *49*, 538–540.
- (8) Cetinkaya, B.; Cetinkaya, E.; Küçükbay, H.; Durmaz, R. Antimicrobial activity of carbene complexes of rhodium(I) and ruthenium(II). *Arzneim. Forsch.* **1996**, *46*, 821–823.
- (9) Durmaz, R.; Küçükbay, H.; Cetinkaya, E.; Cetinkaya, B. Antimicrobial activity of rhodium (I) and ruthenium (II) carbene complexes derived from benzimidazole against *Staphylococcus aureus* isolates. *Turk. J. Med. Sci.* **1997**, *27*, 59–61.
- (10) Skander, M.; Retailliau, P.; Bourrie, B.; Schio, L.; Mailliet, P.; Marinetti, A. N-Heterocyclic carbene-amine Pt(II) complexes, a new chemical space for the development of platinum-based anticancer drugs. *J. Med. Chem.* **2010**, *53*, 2146–2154.
- (11) Sun, R. W.-Y.; Chow, A. L.-F.; Li, X.-H.; Yan, J. J.; Chui, S. S.-Y.; Che, C.-M. Luminescent cyclometalated platinum(II) complexes containing N-heterocyclic carbene ligands with potent in vitro and in vivo anti-cancer properties accumulate in cytoplasmic structures of cancer cells. *Chem. Sci.* **2011**, *2*, 728–736.
- (12) Zhang, J.-J.; Che, C.-M.; Ott, I. Caffeine derived platinum(II) N-heterocyclic carbene complexes with multiple anti-cancer activities. *J. Organomet. Chem.* **2015**, *782*, 37–41.
- (13) Oehninger, L.; Stefanopoulou, M.; Alborzina, H.; Schur, J.; Ludewig, S.; Namikawa, K.; Muñoz-Castro, A.; Köster, R. W.; Baumann, K.; Wölfl, S.; Sheldrick, W. S.; Ott, I. Evaluation of arene ruthenium(II) N-heterocyclic carbene complexes as organometallics interacting with thiol and selenol containing biomolecules. *Dalton Trans.* **2013**, *42*, 1657–1666.
- (14) Gothe, Y.; Marzo, T.; Messori, L.; Metzler-Nolte, N. Cytotoxic activity and protein binding through an unusual oxidative mechanism by an iridium(I)-NHC complex. *Chem. Commun.* **2015**, *51*, 3151–3153.
- (15) Simpson, P. V.; Schmidt, C.; Ott, I.; Bruhn, H.; Schatzschneider, U. Synthesis, cellular uptake and biological activity against pathogenic microorganisms and cancer cells of rhodium and iridium N-heterocyclic carbene complexes bearing charged substituents. *Eur. J. Inorg. Chem.* **2013**, *2013*, 5547–5554.
- (16) McConnell, J. R.; Rananaware, D. P.; Ramsey, D. M.; Buys, K. N.; Cole, M. L.; McAlpine, S. R. A potential rhodium cancer therapy: Studies of a cytotoxic organorhodium(I) complex that binds DNA. *Bioorg. Med. Chem. Lett.* **2013**, *23*, 2527–2531.
- (17) Oehninger, L.; Kuster, L. N.; Schmidt, C.; Munoz-Castro, A.; Prokop, A.; Ott, I. A chemical-biological evaluation of rhodium(I) N-heterocyclic carbene complexes as prospective anticancer drugs. *Chem.—Eur. J.* **2013**, *19*, 17871–17880.
- (18) Geldmacher, Y.; Kitanovic, I.; Alborzina, H.; Bergerhoff, K.; Rubbiani, R.; Wefelmeier, P.; Prokop, A.; Gust, R.; Ott, I.; Wölfl, S.; Sheldrick, W. S. Cellular selectivity and biological impact of cytotoxic rhodium(III) and iridium(III) complexes containing methyl-substituted phenanthroline ligands. *ChemMedChem* **2011**, *6*, 429–439.
- (19) Geldmacher, Y.; Splith, K.; Kitanovic, I.; Alborzina, H.; Can, S.; Rubbiani, R.; Nazif, M. A.; Wefelmeier, P.; Prokop, A.; Ott, I.; Wölfl, S.; Neundorf, I.; Sheldrick, W. S. Cellular impact and selectivity of half-sandwich organorhodium(III) anticancer complexes and their organoiridium(III) and trichloridorhodium(III) counterparts. *JBIC, J. Biol. Inorg. Chem.* **2012**, *17*, 631–646.
- (20) Mollin, S.; Riedel, R.; Harms, K.; Meggers, E. Octahedral rhodium(III) complexes as kinase inhibitors: Control of the relative stereochemistry with acyclic tridentate ligands. *J. Inorg. Biochem.* **2015**, *148*, 11–21.
- (21) Ma, D. L.; Liu, L. J.; Leung, K. H.; Chen, Y. T.; Zhong, H. J.; Chan, D. S.; Wang, H. M.; Leung, C. H. Antagonizing STAT3 dimerization with a rhodium(III) complex. *Angew. Chem., Int. Ed.* **2014**, *53*, 9178–9182.
- (22) Liu, L. J.; Lin, S.; Chan, D. S.; Vong, C. T.; Hoi, P. M.; Wong, C. Y.; Ma, D. L.; Leung, C. H. A rhodium(III) complex inhibits LPS-induced nitric oxide production and angiogenic activity in cellulose. *J. Inorg. Biochem.* **2014**, *140*, 23–28.
- (23) Siu, F.-M.; Lin, I. W.-S.; Yan, K.; Lok, C.-N.; Low, K.-H.; Leung, T. Y.-C.; Lam, T.-L.; Che, C.-M. Anticancer dirhodium(ii,ii) carboxylates as potent inhibitors of ubiquitin-proteasome system. *Chem. Sci.* **2012**, *3*, 1785–1793.
- (24) Leung, C.-H.; Zhong, H.-J.; Chan, D. S.-H.; Ma, D.-L. Bioactive iridium and rhodium complexes as therapeutic agents. *Coord. Chem. Rev.* **2013**, *257*, 1764–1776.
- (25) Geldmacher, Y.; Oleszak, M.; Sheldrick, W. S. Rhodium(III) and iridium(III) complexes as anticancer agents. *Inorg. Chim. Acta* **2012**, *393*, 84–102.
- (26) Kandlioller, W.; Balsano, E.; Meier, S. M.; Jungwirth, U.; Goschl, S.; Roller, A.; Jakupec, M. A.; Berger, W.; Keppler, B. K.; Hartinger, C. G. Organometallic anticancer complexes of lapachol: Metal centre-dependent formation of reactive oxygen species and correlation with cytotoxicity. *Chem. Commun.* **2013**, *49*, 3348–3350.
- (27) Rubbiani, R.; Kitanovic, I.; Alborzina, H.; Can, S.; Kitanovic, A.; Onambe, L. A.; Stefanopoulou, M.; Geldmacher, Y.; Sheldrick, W. S.; Wolber, G.; Prokop, A.; Wölfl, S.; Ott, I. Benzimidazol-2-ylidene gold(I) complexes are thioredoxin reductase inhibitors with multiple antitumor properties. *J. Med. Chem.* **2010**, *53*, 8608–8618.
- (28) Rubbiani, R.; Can, S.; Kitanovic, I.; Alborzina, H.; Stefanopoulou, M.; Kokoschka, M.; Monchgesang, S.; Sheldrick, W. S.; Wölfl, S.; Ott, I. Comparative in vitro evaluation of N-heterocyclic carbene gold(I) complexes of the benzimidazolylidene type. *J. Med. Chem.* **2011**, *54*, 8646–8657.
- (29) Matsuzawa, A.; Ichijo, H. Stress-responsive protein kinases in redox-regulated apoptosis signaling. *Antioxid. Redox Signaling* **2005**, *7*, 472–481.
- (30) Charette, S. J.; Lavoie, J. N.; Lambert, H.; Landry, J. Inhibition of Daxx-mediated apoptosis by heat shock protein 27. *Mol. Cell. Biol.* **2000**, *20*, 7602–7612.
- (31) Mierke, C. T. The role of focal adhesion kinase in the regulation of cellular mechanical properties. *Phys. Biol.* **2013**, *10*, 065005.
- (32) Berven, L. A.; Crouch, M. F. Cellular function of p70S6K: A role in regulating cell motility. *Immunol. Cell Biol.* **2000**, *78*, 447–451.
- (33) Pi, X.; Yan, C.; Berk, B. C. Big mitogen-activated protein kinase (BMK1)/ERK5 protects endothelial cells from apoptosis. *Circ. Res.* **2004**, *94*, 362–369.
- (34) Doble, B. W.; Woodgett, J. R. GSK-3: Tricks of the trade for a multi-tasking kinase. *J. Cell Sci.* **2003**, *116*, 1175–1186.
- (35) Ott, I.; Schmidt, K.; Kircher, B.; Schumacher, P.; Wiglenda, T.; Gust, R. Antitumor-active cobalt-alkyne complexes derived from acetylsalicylic acid: Studies on the mode of drug action. *J. Med. Chem.* **2005**, *48*, 622–629.
- (36) Schur, J.; Manna, C. M.; Deally, A.; Koster, R. W.; Tacke, M.; Tshuva, E. Y.; Ott, I. A comparative chemical-biological evaluation of titanium(IV) complexes with a salen or cyclopentadienyl ligand. *Chem. Commun. (Cambridge, U. K.)* **2013**, *49*, 4785–4787.

- (37) Wang, D.; Lippard, S. J. Cellular processing of platinum anticancer drugs. *Nat. Rev. Drug Discovery* **2005**, *4*, 307–320.
- (38) Holenya, P.; Heigwer, F.; Wolf, S. KOMA: ELISA-microarray calibration and data analysis based on kinetic signal amplification. *J. Immunol. Methods* **2012**, *380*, 10–15.
- (39) Holenya, P.; Kitanovic, I.; Heigwer, F.; Wolf, S. Microarray-based kinetic colorimetric detection for quantitative multiplex protein phosphorylation analysis. *Proteomics* **2011**, *11*, 2129–2133.
- (40) Alborzina, H.; Can, S.; Holenya, P.; Scholl, C.; Lederer, E.; Kitanovic, I.; Wolf, S. Real-time monitoring of cisplatin-induced cell death. *PLoS One* **2011**, *6*, e19714.
- (41) Holenya, P.; Can, S.; Rubbiani, R.; Alborzina, H.; Junger, A.; Cheng, X.; Ott, I.; Wolf, S. Detailed analysis of pro-apoptotic signaling and metabolic adaptation triggered by a N-heterocyclic carbene-gold(I) complex. *Metallomics* **2014**, *6*, 1591–1601.
- (42) Cheng, X.; Holenya, P.; Can, S.; Alborzina, H.; Rubbiani, R.; Ott, I.; Wolf, S. A TrxR inhibiting gold(I) NHC complex induces apoptosis through ASK1-p38-MAPK signaling in pancreatic cancer cells. *Mol. Cancer* **2014**, *13*, 221.
- (43) Romero-Canelon, I.; Salassa, L.; Sadler, P. J. The contrasting activity of iodido versus chlorido ruthenium and osmium arene azo- and imino-pyridine anticancer complexes: Control of cell selectivity, cross-resistance, p53 dependence, and apoptosis pathway. *J. Med. Chem.* **2013**, *56*, 1291–1300.
- (44) Karuvalam, R. P.; Haridas, K. R.; Shetty, S. N. Trimethylsilyl chloride catalyzed synthesis of substituted benzimidazoles using two phase system under microwave conditions, and their antimicrobial studies. *J. Chil. Chem. Soc.* **2012**, *57*, 1122–1125.
- (45) Eren, B.; Erdogan, G. Eco-friendly and efficient synthesis of benzimidazole derivatives using iron oxide modified sepiolite catalyst. *React. Kinet. Mech. Catal.* **2012**, *107*, 333–344.
- (46) Reddy, K. K.; Subba Rao, N. V. Alkylation and aralkylation of N-heterocycles. Part II. Methylation and benzylation of 5 (or 6)-methyl benzimidazoles. *Proc. Ind. Acad. Sci., A* **1969**, *70*, 81–88.
- (47) Rubbiani, R.; Salassa, L.; de Almeida, A.; Casini, A.; Ott, I. Cytotoxic gold(I) N-heterocyclic carbene complexes with phosphane ligands as potent enzyme inhibitors. *ChemMedChem* **2014**, *9*, 1205–1210.
- (48) Navakoski de Oliveira, K.; Andermark, V.; Onambele, L. A.; Dahl, G.; Prokop, A.; Ott, I. Organotin complexes containing carboxylate ligands with maleimide and naphthalimide derived partial structures: TrxR inhibition, cytotoxicity and activity in resistant cancer cells. *Eur. J. Med. Chem.* **2014**, *87*, 794–800.
- (49) Serebryanskaya, T. V.; Lyakhov, A. S.; Ivashkevich, L. S.; Schur, J.; Frias, C.; Prokop, A.; Ott, I. Gold(I) thiotetrazolates as thioredoxin reductase inhibitors and antiproliferative agents. *Dalton Trans* **2015**, *44*, 1161–1169.
- (50) Serebryanskaya, T. V.; Zolotarev, A. A.; Ott, I. A novel aminotriazole-based NHC complex for the design of gold(III) anticancer agents: Synthesis and biological evaluation. *MedChemComm* **2015**, *6*, 1186–1189.